0026-895X/02/6103-533–545$3.00
MOLECULAR PHARMACOLOGY
Copyright © 2002 The American Society for Pharmacology and Experimental Therapeutics
Mol Pharmacol 61:533–545, 2002

Vol. 61, No. 3
1242/967812
Printed in U.S.A.

Channel Blockers Acting at *N*-Methyl-D-aspartate Receptors: Differential Effects of Mutations in the Vestibule and Ion Channel Pore

KEIKO KASHIWAGI, TAKASHI MASUKO,[1] CHRISTOPHER D. NGUYEN, TOMOKO KUNO, IKUKO TANAKA, KAZUEI IGARASHI, and KEITH WILLIAMS

Department of Physiology and Pharmacology, State University of New York Health Science Center, Brooklyn, New York (T.M., K.W.); Department of Pharmacology, University of Pennsylvania School of Medicine, Philadelphia, Pennsylvania (C.D.N., K.W.); Graduate School of Pharmaceutical Sciences, Chiba University, Chiba, Japan (K.K., T.K., I.T., K.I.)

Received July 26, 2001; accepted December 4, 2001

This article is available online at http://molpharm.aspetjournals.org

ABSTRACT

A large number of structurally diverse compounds act as open-channel blockers of NMDA receptors. They may share discrete or overlapping binding sites within the channel. In this study, the effects of mutations in and around the membrane-spanning and pore-forming regions of NMDA receptor subunits were studied with three blockers, MK-801, memantine, and TB-3-4, using recombinant NMDA receptors expressed in *Xenopus laevis* oocytes. Mutations at the critical asparagine residues in the M2 loop of NR1 and NR2B and at a tryptophan residue in M2 of NR2B reduced block by MK-801, memantine, and TB-3-4. Mutations at residues in the pre-M1, M1, M3, post-M3, and post-M4 regions had differential effects on the three blockers. Many mutations in these regions reduced block by MK-801 and TB-3-4 but had no effect on block by memantine. The differential effects on block by memantine and MK-801 are unlikely to be caused by differences in the size of these blockers. Benzyl rings in MK-801 and TB-3-4 may make hydrophobic interactions with aromatic and hydrophobic amino acid residues in the pore. Some mutations in the pre-M1 and M3 regions generated constitutively open channels, characterized by large holding currents. The effects of the various mutants are discussed in the context of models based on the known structure of the pore of the KcsA potassium channel and on previous studies dealing with solvent accessible residues in NMDA receptor subunits as determined by modification after cysteine mutagenesis.

N-Methyl-D-aspartate (NMDA) receptors are ligand-gated ion channels that have structural similarities with the α-amino-3-hydroxy-5-methyl-4-isoxazolepropionic acid (AMPA) and kainate receptors (Dingledine et al., 1999). NMDA receptors have several characteristics that distinguish them from the other glutamate receptors. These include the requirement for two different agonists (glutamate and glycine) to activate the receptor, a high permeability of the channel to Ca^{2+}, and a voltage-dependent block of the channel by Mg^{2+} (Dingledine et al., 1999). NMDA channels are also blocked by a large number of structurally dissimilar organic blockers including ketamine, MK-801, memantine, and various spider toxins and polyamine derivatives (Huettner and Bean, 1988; Collingridge and Lester, 1989; Chen et al., 1992; Igarashi et al., 1997).

With the cloning of cDNAs encoding subunits of glutamate receptors, it has been possible to begin to delineate the structural features that may contribute to various binding sites and/or functional domains of these receptors. The glutamate binding site is formed by two domains (S1 and S2) in the amino terminus and M3–M4 loop of the NR2 subunit, whereas homologous domains in NR1 form the glycine binding site (Kuryatov et al., 1994; Laube et al., 1997; Anson et al., 1998). The amino-terminal domain preceding S1 seems to be a regulatory domain that may contain binding sites for modulators and antagonists such as spermine, protons, ifenprodil, and Zn^{2+} (Masuko et al., 1999; Low et al., 2000; Paoletti et al., 2000). The M2 loop region is a critical determinant of divalent cation permeability and Mg^{2+} block. In particular, asparagine residues in this region form part of a Mg^{2+} binding site and contribute to the selectivity filter of the channel (Dingledine et al., 1999). These asparagine residues, which are in positions analogous to the Q/R sites that control divalent cation permeability of AMPA and kainate channels, have also been found to influence block by organic channel blockers such as MK-801 (Dingledine et al., 1999).

Supported by Unites States Public Health Service grant NS35047 and the Hamaguchi Foundation for the Advancement of Biochemistry, Japan.

[1] Present address: College of Pharmacy, Nihon University, Funabashi, Japan.

ABBREVIATIONS: NMDA, *N*-methyl-D-aspartate; AMPA, α-amino-3-hydroxy-5-methyl-4-isoxazolepropionic acid; TB-3-4, N^1-N^4-N^8-tribenzylspermidine; BAPTA, 1,2-bis(2-aminophenoxy)ethane-*N*,*N*,*N*′,*N*′-tetraacetic acid; NMDG, *N*-methyl-D-glucamine.

There is little information about how other residues in the membrane-spanning and pore-forming regions of NMDA receptors affect block by compounds such as MK-801, memantine, and other organic channel blockers.

In this article, we have studied mutations in the M2 pore-forming loop and in the M1, M3, and M4 membrane-spanning regions and in some adjacent regions. We determined the effects of these mutations on block by three structurally distinct channel blockers: MK-801, memantine, and N^1-N^4-N^8-tribenzyl-spermidine (TB-3-4). MK-801 is a prototypical, high-affinity NMDA channel blocker with a very slow onset and recovery of block (Wong et al., 1986; Huettner and Bean, 1988), whereas memantine is a low-affinity blocker with much faster rates of block and unblock (Chen et al., 1992; Blanpied et al., 1997). Both molecules have quite rigid structures. TB-3-4 is a potent and selective NMDA blocker and is a much larger and more flexible molecule than either MK-801 or memantine (Igarashi et al., 1997). Our results show that block by these three compounds is affected not only by residues in the M2 loop but also by residues toward the extracellular ends of M1, M3, and M4. Notably, mutations in these regions have differential effects on the different blockers. Surprisingly, many mutants that influence block by TB-3-4 also affect MK-801 but have no effect on block by memantine.

Materials and Methods

NMDA Clones and Site-Directed Mutagenesis. The NR1 clone used in these studies is the NR1A variant (Moriyoshi et al., 1991) which lacks the 21-amino acid insert encoded by exon-5. This clone, and some of the NR1 mutants in the M2 and M1–M2 linker region (Sakurada et al., 1993) were gifts from Dr. S. Nakanishi (Institute for Immunology, Kyoto University Faculty of Medicine, Kyoto, Japan). The rat and mouse NR2B clones (Kutsuwada et al., 1992; Monyer et al., 1992) were gifts from Drs. P. H. Seeburg (Center for Molecular Biology, University of Heidelberg, Germany) and M. Mishina (University of Tokyo, Tokyo, Japan).

Site-directed mutagenesis was carried out by the method of Sayers et al. (Sayers et al., 1992) or by the method of Ho et al. (1989) using the polymerase chain reaction. For mutations in NR2B we used the rat NR2B clone or, in some cases, the mouse (ϵ2) NR2B clone containing a 1.7-kilobase *Hin*dIII-*Sph*I fragment of the rat NR2B clone with the mutation of interest (Williams et al., 1998). Mutations were confirmed by DNA sequencing using a Seq 4 × 4 personal sequencing system (Amersham Biosciences) over approximately 300 nucleotides containing the mutation. A list of oligonucleotide primers used for mutagenesis has not been included but is available from the authors upon request.

Numbering of Residues. In NR1 and NR2 subunits, amino acids are numbered from the initiator methionine as in the original paper reporting the sequence of NR1 (Moriyoshi et al., 1991). This differs from the numbering system used in some other laboratories, in which residues are numbered from the start of the mature peptide (Kuner et al., 1996; Beck et al., 1999). In the case of NR1, there is an 18 amino acid signal peptide so, for example, residue NR1(N616) described in this study corresponds to residue NR1(N598) using the alternative numbering scheme (Kuner et al., 1996).

Expression in Oocytes and Voltage-Clamp Recording. The preparation of capped cRNAs and the preparation, injection, and maintenance of oocytes were carried out as described previously (Williams et al., 1993). Oocytes were injected with NR1 plus NR2 cRNAs in a ratio of 1:5 (0.1–4 ng of NR1 plus 0.5–20 ng of NR2). Macroscopic currents were recorded with a two-electrode voltage-clamp using a GeneClamp 500 amplifier (Axon Instruments, Union City, CA) as described previously (Williams, 1993). Electrodes were filled with 3 M KCl and had resistances of 0.4 to 4 MΩ. Oocytes were continuously superfused with a saline solution (100 mM NaCl, 2 mM KCl, 1.8 mM $BaCl_2$, and 10 mM HEPES, pH 7.5) that contained $BaCl_2$ rather than $CaCl_2$ to minimize Ca^{2+}-activated Cl^- currents, and in most experiments oocytes were injected with K^+-BAPTA (100 nl of 40 mM, pH 7.0–7.4) on the day of recording.

Concentration-inhibition curves for antagonists were constructed by using six to nine different concentrations of antagonist for each mutation. Each concentration was tested on at least four oocytes. In many experiments with TB-3-4 and memantine, it was possible to construct an entire concentration-inhibition curve on each oocyte. In those experiments, we calculated the IC_{50} for each individual oocyte, and the reported data are the mean from four or more oocytes. In other experiments, particularly those with MK-801, data were pooled from different oocytes (with a total of four or more oocytes for each concentration of antagonist) to calculate the IC_{50}. Block by MK-801 was very slow, taking several minutes to reach steady state, especially with low concentrations of MK-801, and we did not attempt to measure recovery from block by MK-801 in most oocytes.

Data analysis and curve fitting were carried out using Axograph (Axon Instruments, Foster City, CA) or SigmaPlot (Jandel Scientific, San Rafael, CA) on Macintosh computers. To obtain values for the IC_{50} of antagonists, concentration-inhibition curves were fit to eq. 1:

$$I_{glu+ant}/I_{glu} = 1/[1+([antagonist]/IC_{50})^{n_H}] \quad (1)$$

in which I_{glu} is the response to glutamate and $I_{glu\ +\ ant}$ is the response to glutamate measured in the presence of the antagonist.

To study the voltage-dependence of block, voltage-ramps were constructed by ramping the command signal from −150 mV to +60 or +80 mV over 3 to 4 s. Leak currents, measured in the absence of agonist and blockers, were digitally subtracted. We chose concentrations of blockers that gave a 50 to 80% inhibition at −70 mV at a particular mutant. For analysis of the voltage-dependence of block by TB-3-4 or memantine, data were analyzed using the model of Woodhull (1973) by fitting the data to eq. 2:

$$I_{glu+ant}/I_{glu} = \alpha/[1+([ant]/K_d(0)\exp(z\delta FV/RT))] \quad (2)$$

in which I_{glu} is the control response to glutamate, $I_{glu\ +\ ant}$ is the response to glutamate measured in the presence of the antagonist, α is the fractional recovery from block at depolarized potentials, $K_d(0)$ is the equilibrium dissociation constant of the antagonist at a transmembrane potential of 0 mV, z is the charge of the antagonist, δ is the fraction of the membrane electric field sensed by the blocker at its binding site within that field, F is the Faraday constant, R is the gas constant, and T is the absolute temperature. In the fitting procedure, the parameters α, $K_d(0)$ and $Z\delta$ were free. The α function was included in eq. 2 because, in some cells, the glutamate response showed a small run-down or run-up over time, and the fractional recovery from block at depolarized potentials was often slightly different from 1.0. The inclusion of the α variable improves the fitting procedure, but block by TB-3-4 and memantine does not show a voltage-independent component.

To measure Ba^{2+} permeability, voltage ramps were used to determine current-voltage profiles in extracellular Na^+-saline (saline solution; composition as above) and Ba^{2+}-saline (64 mM $BaCl_2$, 2 mM KCl, 10 mM HEPES, pH 7.5) as described previously (Williams et al., 1998). Values for the reversal potentials (V_{rev}) were calculated by linear regression of data 5 mV either side of an estimated reversal potential. Leak currents were subtracted, and the values of V_{rev} were corrected for small liquid junction potentials (+3 to +8 mV) measured in Ba^{2+}-saline versus Na^+-saline.

Results

Screening Mutations. We initially made a series of individual point mutations in and around the membrane-span-

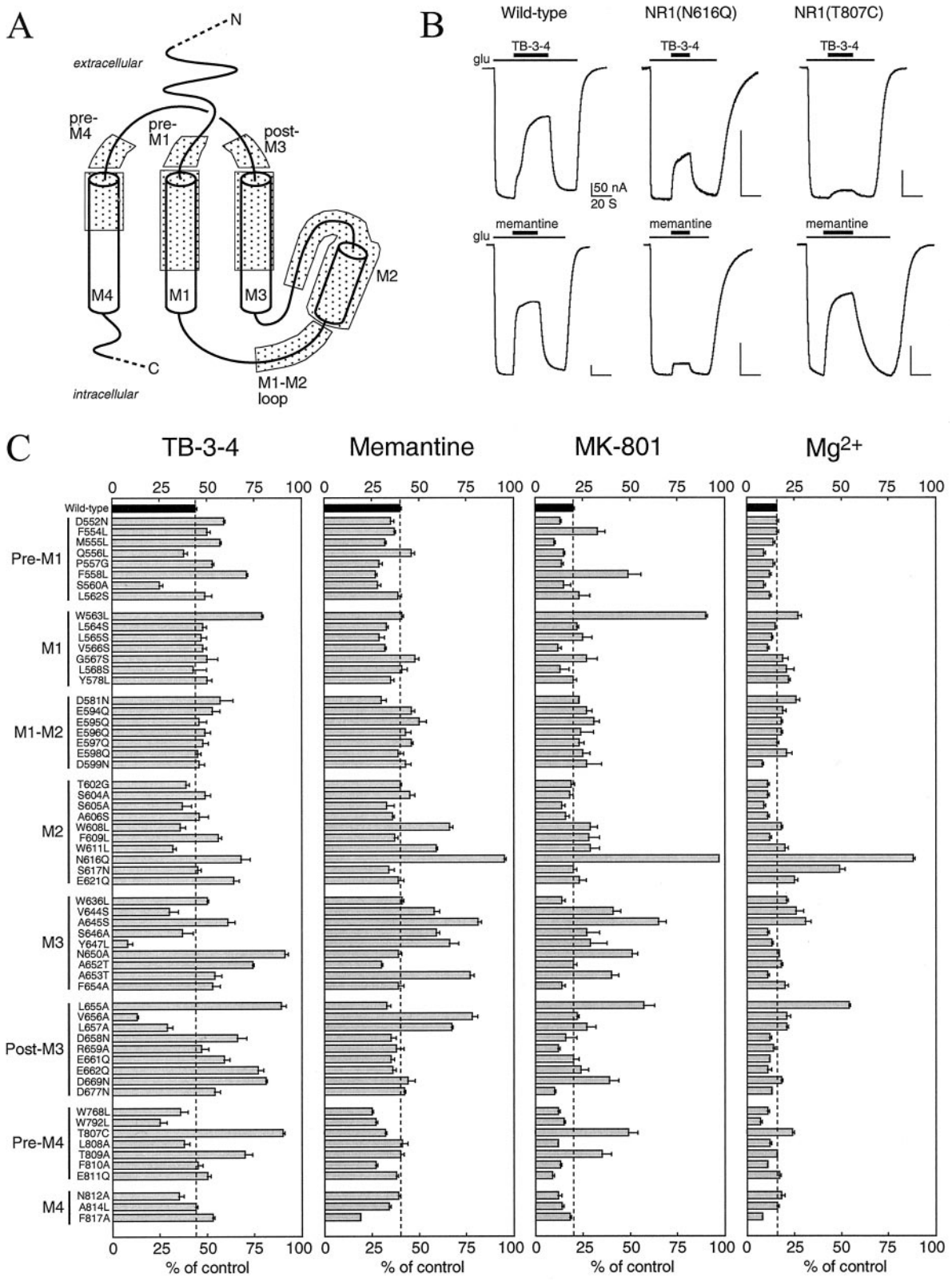

Fig. 1. Screening NR1 mutants. A, schematic of the NR1 subunit, which contains three membrane-spanning domains (M1, M3, and M4), a re-entrant loop (M2), and a large extracellular loop between M3 and M4. The stippled boxes indicate the regions in which mutations were studied. B, examples of experiments designed to screen for effects of mutations on inhibition by channel blockers. The traces are inward currents induced by glutamate (*glu*, 10 μM; with 10 μM glycine) in the absence or presence of blockers in oocytes voltage-clamped at −70 mV. In these examples, the effects of 0.3 μM TB-3-4 (top row) and 1 μM memantine (bottom row) were determined at NR1/NR2B receptors containing wild-type NR1, NR1(N616Q), and NR1(T807C) subunits. All horizontal scale bars are 20 s, and all vertical scale bars are 50 nA. C, the effects of TB-3-4 (0.3 μM), memantine (1 μM), MK-801 (30 nM), and Mg^{2+} (100 μM) were determined at NR1/NR2B receptors containing wild-type and mutant subunits using protocols similar to those shown in B. Currents measured in the presence of blockers are expressed as a percentage of control currents.

ning and pore-forming loop regions of the NR1 subunit. The mutants were constructed in most cases to alter the functional side chain, for example by neutralizing the charge (E-to-Q, D-to-N), removing an aromatic ring (W-to-L, Y-to-L) or removing a hydroxyl group (S-to-A, T-to-A). The regions that were studied are shown schematically in Fig. 1A. We screened each mutation by measuring block using a single concentration of TB-3-4, memantine, and MK-801 at NR1/NR2B receptors (Fig. 1). In these experiments, we also studied the effects of mutations on block by 100 μM Mg^{2+}.

As expected, an NR1(N616Q) mutation in the M2 loop reduced block by all four compounds (Fig. 1C). We found that a number of other mutations, particularly in the pre-M1, M1, M3, post-M3, and pre-M4 regions, reduced inhibition by the organic channel blockers. However, some of these mutants had differential effects on the different blockers. For example, mutations W563L in the M1 region, N650A in the M3 region, and T807C in the pre-M4 region reduced the effects of TB-3-4 and MK-801 but had no effect on block by memantine (Fig. 1C). We subsequently studied in detail mutations at residues that affected block by one or more of the three organic channel blockers. The results from those studies are described below. Only mutations at N616, S617, and L655 had pronounced effects on block by Mg^{2+} (Fig. 1C). The effects of mutations at N616 and S617 have been studied in detail by other investigators (Kuner et al., 1996; Wollmuth et al., 1998a,b), and we did not carry out further studies of Mg^{2+} block. Nonetheless, the profile for Mg^{2+} shown in Fig. 1C is clearly a useful comparison with the three other blockers that were studied; there are many more mutations that influence block by TB-3-4, MK-801, and memantine than by Mg^{2+}. In addition to the mutants listed on Fig. 1, we made two mutants at position T648, but these mutants, when coexpressed with NR2B, generated large leak currents in the oocytes, presumably because of formation of constitutively open channels. This is discussed below.

In the following sections, we describe the effects of the various key NR1 mutants identified in Fig. 1. For each of the

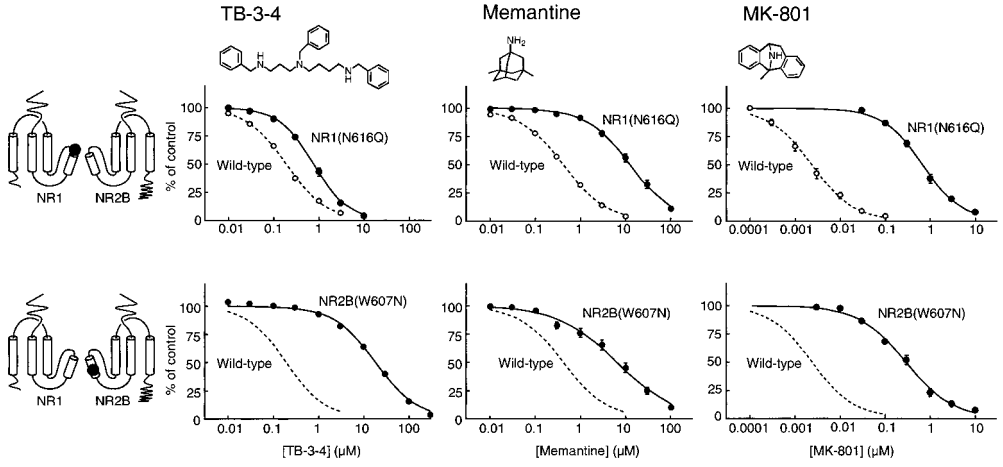

Fig. 2. Effects of mutations in the M2 region. Concentration-inhibition curves for TB-3-4, memantine, and MK-801 at wild-type and mutant NR1/NR2B receptors were constructed using four or more oocytes for each concentration of blocker. Data for wild-type receptors (○) are shown only in the top, and the fitted curves for wild-type receptors are shown by broken lines. Data are currents measured in the presence of blocker expressed as a percentage of the control current measured in the absence of the blocker. The structures of the three blockers are shown at the top, and the relative positions of the mutations are shown schematically at the left side.

TABLE 1

Effects of NR1 and NR2B mutants in the M2 loop region on block by TB-3-4, memantine, and MK-801

Values of the IC_{50} were determined from concentration-inhibition curves, and values of the $K_d(0)$ and $z\delta$ were determined using voltage ramps analyzed with the Woodhull model of voltage-dependent block.

Mutant	TB-3-4						Memantine						MK-801	
	IC_{50}	Mutant/WT[a]	$K_d(0)$	Mutant/WT[a]	$z\delta$	Mutant/WT[a]	IC_{50}	Mutant/WT[a]	$K_d(0)$	Mutant/WT[a]	$z\delta$	Mutant/WT[a]	IC_{50}	Mutant/WT[a]
	μM		μM				μM		μM				μM	
Wild-Type NR1/NR2B	0.20		8.8		1.38		0.46		7.1		0.89		0.002	
NR1(N616Q)/NR2B	0.73	4	12	1	1.15	0.8	12.68	28	151	21	0.87	1.0	0.66	330
NR1(N616G)/NR2B	0.36	2	N.D.		N.D.		3.90	8	36	5	0.90	1.0	0.09	45
NR1(N616W)/NR2B	0.10	1	N.D.		N.D.		4.67	10	N.D.		N.D.		0.53	265
NR1(N616R)/NR2B	176	861	N.D.		N.D.		>300[b]	>600	N.D.		N.D.		22	11,000
NR1/NR2B(N615Q)	0.59	3	18	2	1.47	1.1	4.31	9	49	7	0.81	0.9	1.0	500
NR1/NR2B(N616Q)	1.3	6	98	11	1.77	1.3	2.18	5	28	4	0.79	0.9	0.61	305
NR1/NR2B(W607L)	7.4	36	N.D.		N.D.		7.81	17	59	8	0.77	0.9	0.22	110
NR1/NR2B(W607N)	18	88	N.D.		N.D.		6.44	14	39	6	0.57	0.6	0.29	145
NR1/NR2B(W607A)	4.4	21	N.D.		N.D.		1.88	4	34	5	0.69	0.8	0.11	55
NR1/NR2B(W607Y)	0.55	3	15	2	1.17	0.8	0.58	1	6.1	1	0.85	1.0	0.01	5
NR1/NR2B(W607F)	0.39	2	13	2	1.37	1.0	0.55	1	6.0	1	0.85	1.0	0.001	1
NR1/NR2B(W607N/N616Q)	25	125	N.D.		N.D.		6.05	13	N.D.		N.D.		3	1,500
NR1(N616Q)/NR2B(W607N)	23	114	N.D.		N.D.		59.00	128	N.D.		N.D.		10	5,000
NR1(N616G)/NR2B(W607A)	15	74	N.D.		N.D.		4.47	10	N.D.		N.D.		0.53	265
NR1(N616G)/NR2B(W607N)	9.3	45	N.D.		N.D.		18.90	41	N.D.		N.D.		1.8	900
NR1(N616Q)/NR2B(N615Q)	3.8	18	N.D.		N.D.		20.10	44	280	40	0.92	1.0	18	9,000
NR1(N616Q)/NR2B(N616Q)	0.92	5	N.D.		N.D.		6.98	15	64	9	0.85	1.0	0.37	185

N.D., not determined.
[a] Ratio of the IC_{50}, $K_d(0)$, or $z\delta$ for mutant/wild-type.
[b] 300 μM memantine inhibits NR1(N616R)/NR2B channels by 32 ± 1%.

interesting mutants, we constructed concentration-inhibition curves for TB-3-4, memantine, and MK-801 to quantify the effect of each mutation on each blocker. For TB-3-4 and memantine we also constructed voltage ramps and analyzed them using the Woodhull model of voltage-dependent block to obtain values for the $K_d(0)$ and the apparent valence ($z\delta$). In some cases, we made additional mutations at particular positions in NR1 and/or studied mutations at equivalent positions in the NR2B subunit. We have divided the presentation of these results into two sections. One section deals with the M2 loop region (which has previously been studied in most detail with respect to channel blockers), and the other section deals with M1, M3, M4, and adjacent regions.

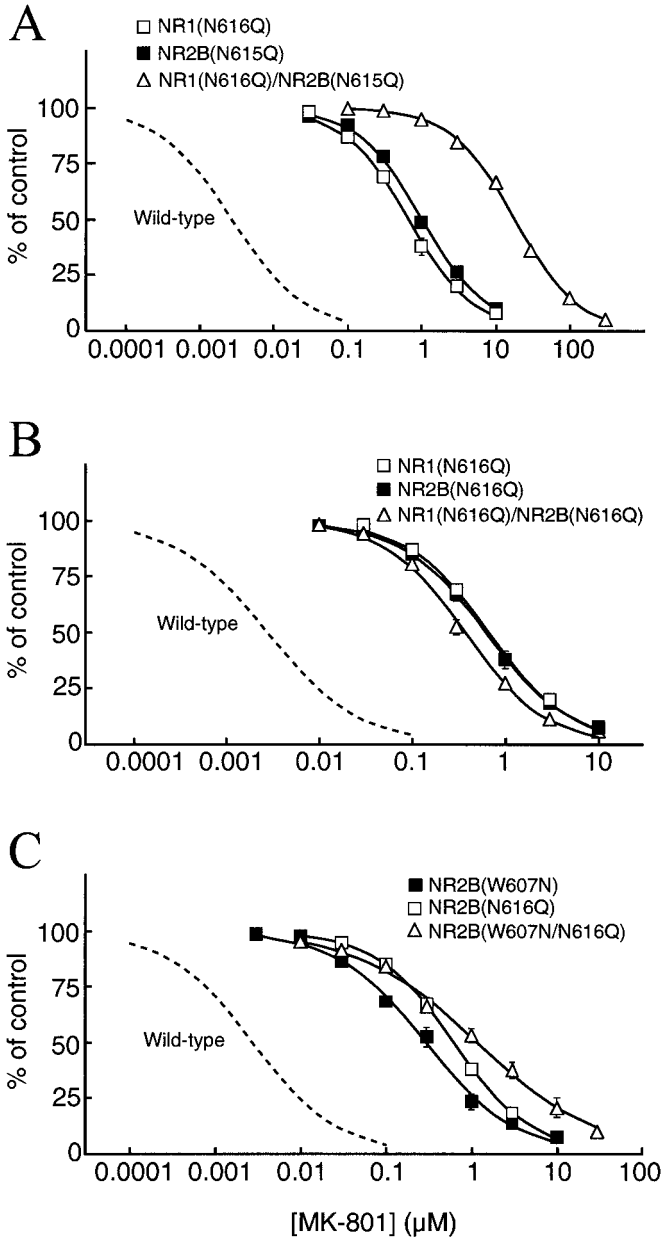

Fig. 3. Effects of mutations in the M2 regions of NR1 and NR2B. Concentration-inhibition curves for MK-801 at wild-type and mutant NR1/NR2B receptors were constructed using four or more oocytes for each concentration of MK-801. The data for wild-type receptors are not shown, but the fitted curves for wild-type receptors are shown by broken lines. Data are currents measured in the presence of MK-801 expressed as a percentage of the control current measured in the absence of MK-801.

The M2 Loop/Pore-Forming Region. The M2 loop of NR1 contains an asparagine (N616) that has previously been shown to influence divalent cation permeability and block by Mg^{2+}, MK-801, and other channel blockers (Dingledine et al., 1999). An N-to-Q mutation at this position reduced block by TB-3-4, memantine, and MK-801. The NR2B subunit contains two asparagines (N615 and N616) at positions equivalent to N616 and S617 in NR1, and we studied mutations at both N residues in NR2B. In the M2 region of NR1, mutations at two tryptophan residues (W608 and W611) had small effects on block by memantine (Fig. 1C). We have previously found that mutations at NR1(W608) had little or no effect on Mg^{2+} block, whereas mutations at NR2B(W607), a position equivalent to NR1(W608), had dramatic effects on Mg^{2+} block (Williams et al., 1998). In light of this, we studied the effects of NR2B(W607) mutations on block by TB-3-4, memantine, and MK-801. Thus, the studies of the M2 region are focused on NR1(N616), NR2B(N615), NR2B(N616), and NR2B(W607).

N-to-Q mutations at any of the three critical N residues in NR1 and NR2B reduced the potencies of TB-3-4, memantine, and MK-801 (Fig. 2, Table 1). The largest effects of the N-to-Q mutations were on block by MK-801, with only modest effects on TB-3-4. An NR2B(W607N) mutation, in the M2 region of NR2B, also greatly reduced the potencies of all three blockers (Fig. 2, Table 1). We studied a number of different mutations at this position and found that substitutions of W-to-N, W-to-L, or W-to-A all greatly reduced the potencies of the blockers whereas W-to-Y or W-to-F mutants had little or no effect (Table 1). Thus, an aromatic residue at position NR2B(W607) seems to be important for block by the organic channel blockers, as has previously been seen with Mg^{2+} (Williams et al., 1998).

We carried out experiments to determine whether the effects of mutations at NR1(N616) were additive with those of mutations at NR2B(N615) and NR2B(N616). If the effects of any two mutants are not additive, this would suggest that the residues together form a binding site that is ablated by mutation of either residue. The results for MK-801 are shown

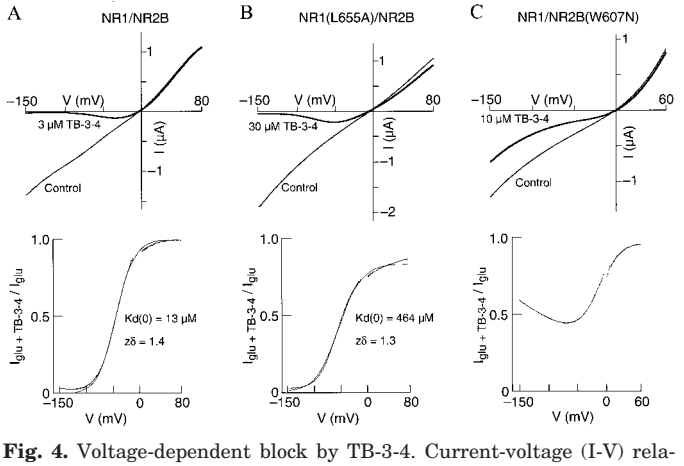

Fig. 4. Voltage-dependent block by TB-3-4. Current-voltage (I-V) relationships were measured by voltage ramps in the absence (control) and presence of TB-3-4 at receptors containing wild-type (A), L655A (B), and W607N(C) NR1 mutants. Bottom, currents measured in the presence of TB-3-4 ($I_{glu+TB-3-4}$) are expressed as a fraction of the control current (I_{glu}). Data around the reversal potential have been masked. The solid lines for NR1/NR2B and NR1(L655A)/NR2B are fits to Woodhull model (eq. 2). Note the incomplete block at NR1/NR2B(W607N) receptors and the apparent reversal of the slope at very negative membrane potentials.

in Fig. 3A and B, and similar results were seen with TB-3-4 (Table 1). In the case of NR2B(N615Q), a much larger increase in IC_{50} was seen with NR1(N616Q)/NR2B(N615Q) than with either individual mutation (Fig. 3A, Table 1). In the case of NR2B(N616Q), the combined effects of the NR1(N616Q)/NR2B(N616Q) mutations were not greater than those of the individual mutations (Fig. 3B, Table 1). This suggests that the NR1(N616) and NR2B(N616) residues make equal, nonadditive contributions to the binding site for these blockers whereas the NR2B(N615) residue makes an additional contribution.

Experiments were also carried out to determine whether the effects of mutations at NR2B(W607) were additive with those of mutations at NR1(N616) and at NR2B(N616). The profile for the various antagonists at receptors expressed from combinations of NR1(N616) mutants and NR2B(W607) mutants was complex, but a notable finding was that the effects of combining mutants at NR1(N616) and NR2B(W607) were generally greater than effects seen with each individual mutant (Table 1). We studied a double mutant, NR2B(W607N/N616Q), and found that the effect of this mutant was not greater than that of either of the single mutants NR2B(W607) and NR2B(N616) (Fig. 3C, Table 1). Thus, the effects of mutations at W607 and N616 within the same subunit (NR2B) are not additive.

We studied the effects of mutations on the voltage-dependence of block by TB-3-4 and memantine using voltage ramps analyzed with the Woodhull model of voltage-dependent block. With wild-type receptors and with many of the mutants that we studied, TB-3-4 and memantine produced a complete or near complete block at very hyperpolarized potentials. Examples are shown for TB-3-4 at wild-type receptors and at NR1(L655A)/NR2B receptors in Fig. 4, A and B. Data from these experiments were fit to the Woodhull model (Fig. 4, A and B, bottom) to obtain values for the $K_d(0)$ and $z\delta$ for each blocker. However, some mutations in the M2 loop region had dramatic effects on the current-voltage profile, with block becoming more pronounced as the cell was hyperpolarized, but with a reversal of the slope conductance and an apparent relief of block at very hyperpolarized potentials. An example is shown in Fig. 4C for TB-3-4 at NR2B(W607N). This type of profile was seen with some mutants at NR1(N616), NR2B(W607), and with combinations of those mutants. We did not attempt to fit data from those mutants to the Woodhull model. The relief of block at very negative membrane potentials presumably reflects permeation of TB-3-4 and memantine through the channels in these mutant receptors. The effects are reminiscent of the effects of some N616 and W607 mutants on block by N^1-dansyl-spermine and Mg^{2+}, in which the mutants increased permeation of the

TABLE 2

Effects of NR1 and NR2B mutants in and around the M1, M3, and M4 regions on block by TB-3-4, memantine, and MK-801

Values of the IC_{50} were determined from concentration-inhibition curves, and values of the $K_d(0)$ and $z\delta$ were determined using voltage ramps analyzed with the Woodhull model of voltage-dependent block.

	Mutant	TB-3-4						Memantine						MK-801	
		IC_{50}	Mutant/WT[a]	$K_d(0)$	Mutant/WT[a]	$z\delta$	Mutant/WT[a]	IC_{50}	Mutant/WT[a]	$K_d(0)$	Mutant/WT[a]	$z\delta$	Mutant/WT[a]	IC_{50}	Mutant/WT[a]
		μM		μM				μM		μM				μM	
	Wild-Type NR1/NR2B	0.20		8.8		1.38		0.46		7.1		0.89		0.002	
Pre-M1	NR1(F558L)/NR2B	0.83	4	27	3	1.52	1.1	0.40	1	2.4	0.3	0.84	0.9	0.024	12
M1	NR1(W563L)/NR2B	2.1	10	52	6	1.30	0.9	0.52	1	3.9	1	0.74	0.8	0.037	19
	NR1(W563A)/NR2B	1.6	8	100	11	1.52	1.1	0.38	1	1.0	0.1	0.51	0.6	0.098	49
	NR1(W563Y)/NR2B	0.14	1	5.7	1	1.39	1.0	0.45	1	11	2	0.92	1.0	0.001	1
	NR1(W563F)/NR2B	0.15	1	7.8	1	1.47	1.1	0.46	1	6.7	1	0.87	1.0	0.003	2
M1	NR1/NR2B(W559L)	12	59	569	65	1.41	1.0	0.32	1	N.D.		N.D.		0.66	330
	NR1/NR2B(W559Y)	0.52	3	26	3	1.55	1.1	0.31	1	3.0	0.4	0.83	0.9	0.043	22
	NR1/NR2B(W559F)	2.7	13	174	20	1.59	1.2	0.36	1	2.1	0.3	0.69	0.8	0.059	30
M3	NR1(A645S)/NR2B	0.23	1	11	1	1.52	1.1	2.6	6	67	9	1.04	1.2	0.11	55
	NR1(A645T)/NR2B	0.61	3	34	4	1.57	1.1	0.56	1	12	2	1.01	1.1	0.079	40
M3	NR1(Y647L)/NR2B	0.05	0.3	N.D.		N.D.		2.1	4	10	1	1.01	1.1	0.005	3
	NR1(Y647A)/NR2B	0.22	1	33	4	1.77	1.3	0.20	0.4	0.9	0.1	0.50	0.6	0.027	14
	NR1(Y647F)/NR2B	0.08	0.4	3.6	0.4	1.35	1.0	1.0	2	23	3	0.87	1.0	0.005	3
	NR1(Y647W)/NR2B	0.21	1	11	1	1.39	1.0	0.88	2	8.4	1	0.86	1.0	0.006	3
M3	NR1/NR2B(Y646L)	1.9	9	50	6	1.34	1.0	0.47	1	6.2	1	0.75	0.8	0.022	11
M3	NR1(N650A)/NR2B	5.9	29	181	21	1.20	0.9	0.54	1	5.9	1	0.88	1.0	0.013	7
	NR1(N650D)/NR2B	0.02	0.1	1.2	0.1	1.69	1.2	0.56	1	21	3	0.99	1.1	0.013	7
	NR1(N650Q)/NR2B	0.53	3	35	4	1.41	1.0	0.45	1	7.4	1	0.99	1.1	0.004	2
	NR1/NR2B(N649Q)	5.7	28	298	34	1.31	0.9	0.45	1	4.1	1	0.90	1.0	0.022	11
M3	NR1(A652T)/NR2B	1.1	6	71	8	1.69	1.2	0.43	1	3.5	1	0.78	0.9	0.004	2
	NR1(A653T)/NR2B	0.10	1	4.5	1	1.46	1.1	1.7	4	61	9	1.20	1.3	0.010	5
	NR1(A653V)/NR2B	0.29	1	30	3	1.52	1.1	0.65	1	11	2	1.03	1.2	0.003	2
Post-M3	NR1(L655A)/NR2B	9.1	45	407	46	1.32	1.0	0.61	1	2.5	0.4	0.93	1.0	0.034	17
	NR1(L655V)/NR2B	1.56	8	52	6	1.45	1.1	0.65	1	8.6	1	1.01	1.1	0.003	2
Post-M3	NR1(V656A)/NR2B	0.05	0.3	4.3	1	1.61	1.2	1.77	4	64	9	1.08	1.2	0.003	2
Post-M3	NR1(E662Q)/NR2B	0.33	2	23	3	1.39	1.0	0.40	1	5.2	1	0.96	1.1	0.003	2
Post-M3	NR1(D669N)/NR2B	1.21	6	27	3	1.51	1.1	0.40	1	3.7	1	0.90	1.0	0.014	7
Post-M3	NR1/NR2B(D668N)	1.1	6	71	8	1.56	1.1	0.32	1	2.4	0.3	0.69	0.8	0.030	15
Pre-M4	NR1(T807C)/NR2B	7.3	36	969	110	1.70	1.2	0.45	1	2.2	0.3	0.66	0.7	0.030	15
	NR1(T807S)/NR2B	0.92	5	43	5	1.51	1.1	0.43	1	9.1	1	1.01	1.1	0.003	2
	NR1(T807V)/NR2B	0.11	1	6.4	1	1.64	1.2	0.51	1	10	1	1.05	1.2	0.003	2
Pre-M4	NR1(T809A)/NR2B	0.42	2	28	3	1.49	1.1	0.61	1	7.4	1	0.92	1.0	0.003	2
Pre-M4	NR1(T809S)/NR2B	0.15	1	15	2	1.48	1.1	0.49	1	11	2	0.93	1.0	0.003	2

N.D., not determined.

[a] Ratio of the IC_{50}, $K_d(0)$, or $z\delta$ for mutant/wild-type.

blockers (Chao et al., 1997; Williams et al., 1998). This may have been caused by an increase in the size of the narrow constriction of the channel pore, allowing the normally impermeant or very poorly permeable blockers to permeate when the driving force is sufficiently high. For mutants at which we could determine values for the $K_d(0)$ and $z\delta$ of the blockers, the mutants increased the $K_d(0)$ but had little or no effect on $z\delta$ (Table 1).

The M1, M3, and M4 Domains. The effects of mutations in these regions are listed in Table 2 and are summarized (together with the effects on mutations in the M2 region) in Fig. 5. Mutations that produced a 3-fold change in IC_{50} (shaded areas on Fig. 5) were considered to be significant. In the pre-M1 and M1 regions of NR1, an F558L mutation had a modest effect on block by TB-3-4 and MK-801 without affecting memantine (Table 2, Fig. 5), whereas mutations at W563 had larger effects on block by TB-3-4 and MK-801, again with no effect on block by memantine (Fig. 6B, top, and Table 2).

In the M3 and post-M3 regions, mutations at residues Y647, A652, A653, V656, E662, and D669 in NR1 had modest effects. More pronounced effects were seen with mutations at A645, N650, and L655 in NR1 (Fig. 6, Table 2). In the M4 and post-M4 regions, mutations at T807 in NR1 had large effects on block by TB-3-4 and MK-801 but little or no effect on block by memantine (Fig. 6B, Table 2). This was similar to the effects of mutants at W563 in M1 and N650 in M3 (Fig. 6B).

We studied a number of different mutations (W-to-L, -A, -Y, and -F) at NR1(W563). The results are shown in Fig. 7A and Table 2. The W-to-L or W-to-A mutations had large effects on block by TB-3-4 and MK-801, increasing the IC_{50} and $K_d(0)$ by 8- to 49-fold, whereas the W-to-Y and W-to-F mutations had no effect. None of the mutations altered block by memantine (Table 2). We also studied mutations at the equivalent position, W559, in the M1 region of the NR2B subunit. Similar to the NR1(W563L) mutation, an NR2B(W559L) mutation greatly reduced inhibition by TB-3-4 and MK-801 (increasing the values of IC_{50} and $K_d(0)$ by 59- to 330-fold) but had no effect on block by memantine (Fig. 5, Table 2). A W-to-A mutation at NR2B(W559) was nonfunctional when coexpressed with NR1. Mutations of W559 to Y or F had smaller effects than the W-to-L mutation on block by TB-3-4 and MK-801. In all cases, the magnitude of the change in $K_d(0)$ for TB-3-4 was similar to that for the change

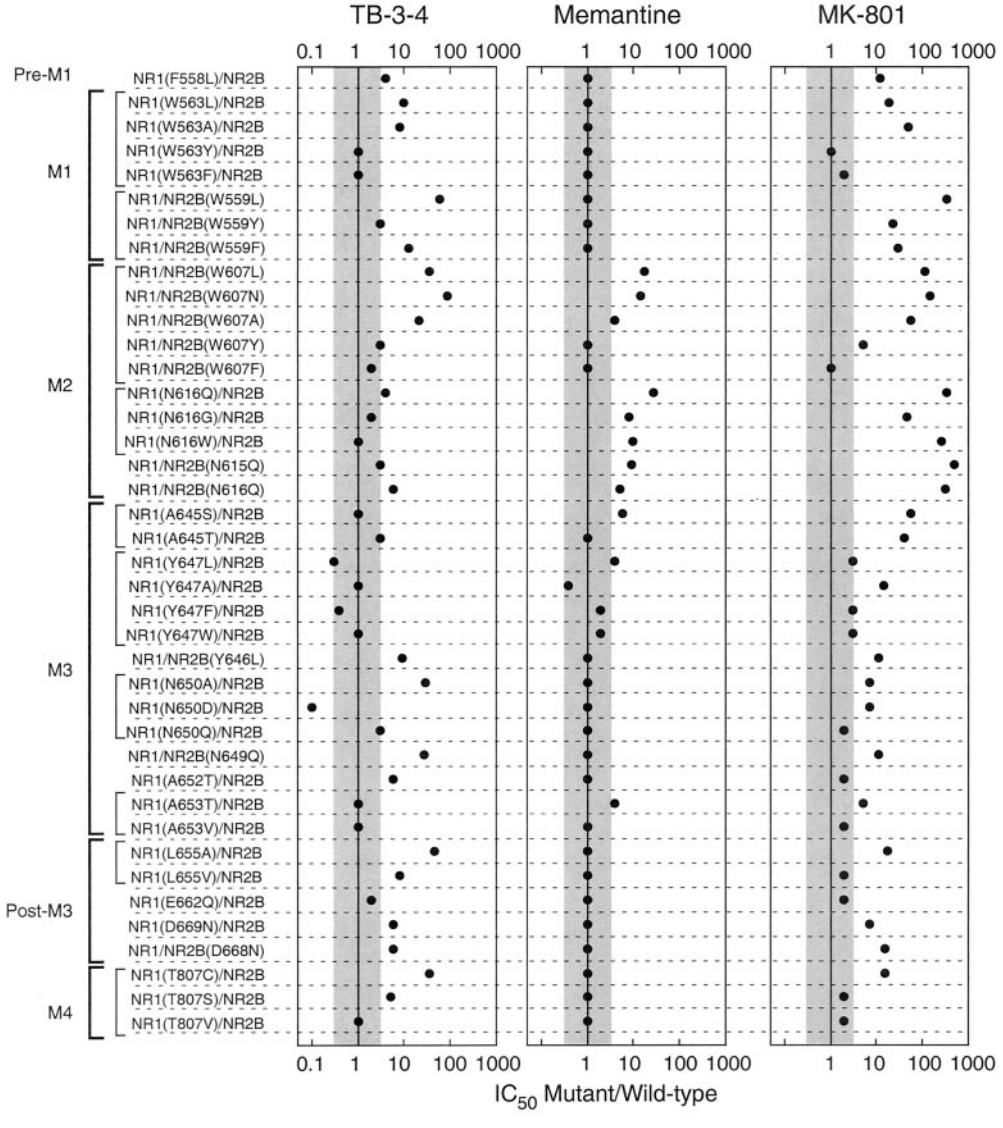

Fig. 5. Summary of the effects of mutants on the potencies of channel blockers. The IC_{50} values for channel blockers at each mutant are expressed relative to wild-type receptors. Data are from concentration-inhibition curves and are re-plotted from Tables 1 and 2. The shaded area represents a 3-fold change in potency. Different mutations at the same position are grouped by thin vertical bars on the left. Thick vertical bars group residues within the various regions (M1, M2, M3, etc.).

in IC_{50}. Taken together, these data suggest residues NR1(W563) and NR2B(W559) influence binding of TB-3-4 and MK-801, and that the aromatic ring of the tryptophan (also found in Y and F but not in L or A residues) is an important determinant of block in wild-type channels.

At position NR1 (N650), an N-to-A mutation increased the IC_{50} and $K_d(0)$ values of TB-3-4 by 21- to 29-fold, whereas an N-to-D mutation had the opposite effect, reducing the values by 10-fold. An N-to-Q mutation at NR1(N650) had little effect (Table 2; Fig. 7B). Mutations at this position had smaller effects on block by MK-801 (2- to 7-fold) than on block by TB-3-4 and had no effect on memantine. If the amino groups of MK-801 and memantine (which have only one amino group each) and one of the three amino groups of TB-3-4 bind at the *N*-site residues in M2, it is conceivable that the side chain of N650 in M3 interacts with another amino group on TB-3-4. This could explain the decrease in potency seen with the N-to-A mutation and the increase in potency seen with the N-to-D mutation at NR1(N650). A mutation at the equivalent position in NR2B, NR2B(N649), also reduced block by TB-3-4.

A large decrease in affinity was seen with a T-to-C mutation but not with T-to-S or T-to-V mutations at NR1(T807) (Fig. 7C). The lack of effect of the S and V mutations suggests that neither the size nor the hydrophobicity of the side chain at this position is the key determinant. A T-to-A mutation at this position gave rise to receptors that generated only very small currents (1–5 nA).

Mutations That Generate Constitutively Open Channels. In initial experiments in which we screened a large number of mutations in the NR1 subunit, we found that oocytes expressing NR1/NR2B receptors with a T-to-A or T-to-S mutation at T648 (located in M3) had very large holding currents when voltage-clamped at −70 mV. An example is shown in Fig. 8A. Application of glutamate and glycine to these mutants did induce inward currents, but the currents were often irreversible on wash-out of the agonists (data not shown), and we did not attempt to study the effects of TB-3-4,

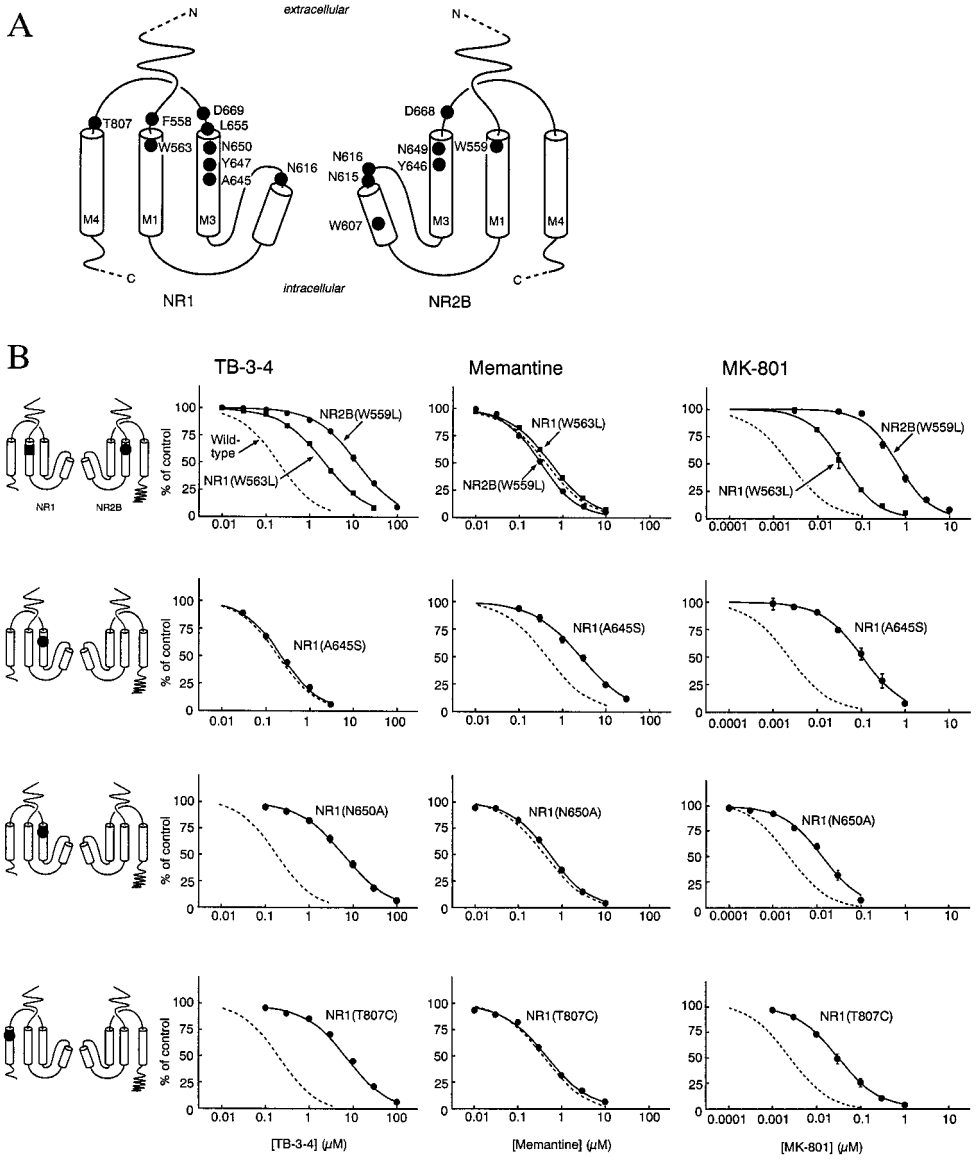

Fig. 6. Effects of mutations in and adjacent to the M1, M3, and M4 regions of NR1 and NR2B. A, schematic showing the positions of the key residues described in this figure and in Tables 1 and 2 and Fig. 5. B, concentration-inhibition curves for TB-3-4, memantine, and MK-801 at wild-type and mutant NR1/NR2B receptors were constructed using four or more oocytes for each concentration of blocker. For clarity, the data for wild-type receptors are not shown, but the fitted curves for wild-type receptors are shown by broken lines. Data are currents measured in the presence of blocker expressed as a percentage of the control current measured in the absence of the blocker. The relative positions of the mutations are shown schematically at the left side.

memantine, and MK-801 at the T648 mutants. We reasoned that the large holding currents required to voltage-clamp cells expressing NR1(T648) mutants may be due to the expression of constitutively open channels in receptors containing these mutants. If this were the case, replacing extracellular Na^+ (the main charge carrier) with the large impermeant cation *N*-methyl-D-glucamine (NMDG) should reduce the currents. We also hypothesized that extracellular Mg^{2+}, applied in the absence of agonists, would block these constitutively open channels, provided that the mutation does not disrupt the Mg^{2+} binding site. To test this, we studied the effects of substituting NMDG for Na^+ in the extracellular solution, and we also studied the effects of extracellular Mg^{2+}. Substitution of Na^+ by NMDG or the addition of 100 μM Mg^{2+} greatly reduced the holding currents in cells expressing receptors containing NR1(T648) mutants but had little effect on wild-type receptors (Fig. 8, A and C). In light of this, we also examined the effects of NMDG and Mg^{2+} at many of the other key mutations that we had characterized and at some adjacent and nearby residues (Fig. 8C). Only mutations at Q556, P557, T648, and L657 in NR1 produced holding currents that were larger than wild-type and were sensitive to NMDG and Mg^{2+} (Fig. 8, B and C). An NR2B(N649D) mutation had a similar effect. In all cases the increased holding current, and consequent reduction by NMDG or Mg^{2+}, were modest compared with the effects seen with NR1(T648) mutants.

Effects of Mutations on Permeability of Ba^{2+}. Mutations at the N residues in the M2 loop and at NR2B(W607) have previously been shown to affect permeability of divalent cations including Ca^{2+} and Ba^{2+} (Williams et al., 1998; Dingledine et al., 1999). We carried out experiments to determine whether the key residues identified in this study affect permeability of Ba^{2+}. Reversal potentials were measured in extracellular solutions that contained Na^+ or Ba^{2+} as the main charge carrier. The shift in reversal potential between Na^+ and Ba^{2+} is an index of the permeability of the channel to Ba^{2+}. We used Ba^{2+} rather than Ca^{2+} in these studies to minimize Ca^{2+}-activated Cl^- conductances (Leonard and Kelso, 1990). At wild-type NR1/NR2B receptors, the reversal potentials were -1.6 ± 0.3 mV (Na^+) and $+21.1 \pm 0.6$ mV (Ba^{2+}). As shown in Fig. 9, mutations at NR1(N616) and NR2B(W607) in the M2 loop had characteristic effects on

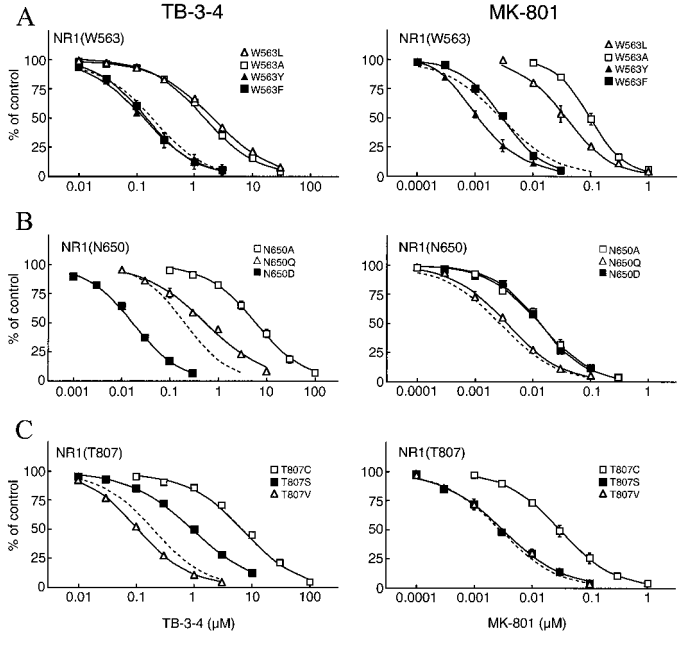

Fig. 7. Effects of different mutations at individual residues. A number of different mutations (e.g., W-to-L, W-to-A, W-to-Y, and W-to-F) were studied at residues W563 (A), N650 (B), and T807 (C) in the NR1 subunit. Concentration-inhibition curves for TB-3-4 and MK-801 at wild-type and mutant NR1/NR2B receptors were constructed using four or more oocytes for each concentration of blocker. For clarity, the data for wild-type receptors are not shown, but the fitted curves for wild-type receptors are shown by broken lines. Data are currents measured in the presence of blocker expressed as a percentage of the control current measured in the absence of the blocker.

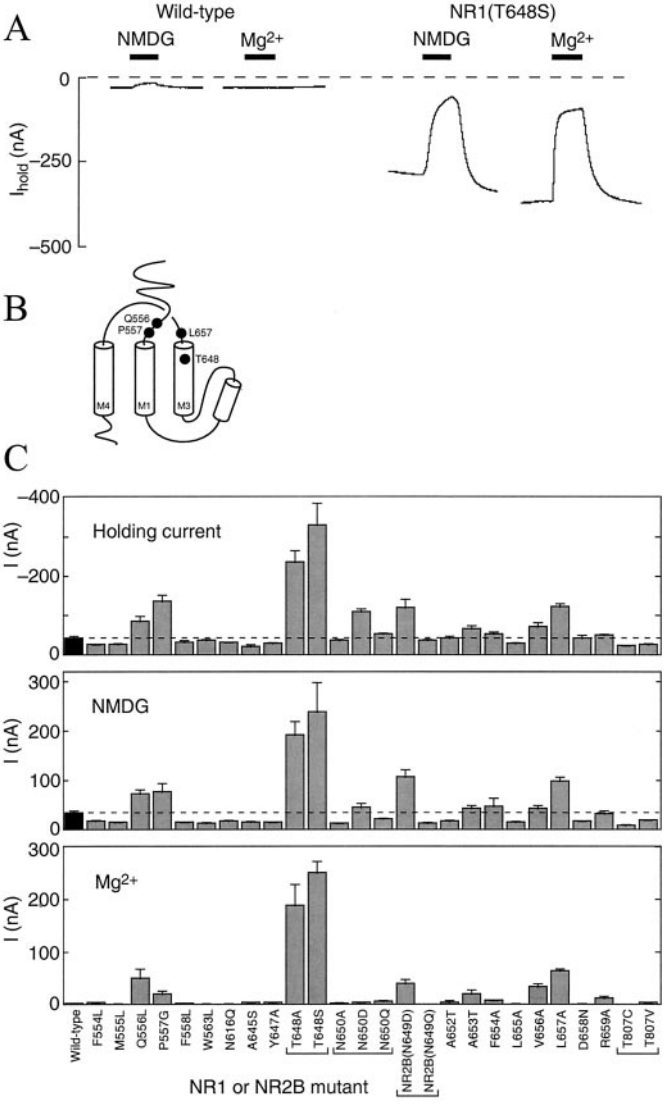

Fig. 8. Residues that may influence gating of NMDA receptors. A, holding currents were recorded in oocytes expressing wild type NR1/NR2B and NR1(T648S)/NR2B receptors and voltage-clamped at -70 mV. Buffer containing 100 mM NMDG (substituted for extracellular Na^+) or 100 μM Mg^{2+} was applied during the times indicated by horizontal bars. Note that NMDG substitution and application of Mg^{2+} was carried out in the *absence* of agonists. B, schematic of the NR1 subunit showing positions of residues at which NMDG and Mg^{2+} reduced the holding current. C, holding current (in oocytes voltage-clamped at -70 mV), and effects of NMDG and Mg^{2+} on the holding current in NR1/NR2B receptors containing wild-type and mutant subunits. The effects of NMDG and Mg^{2+} were determined using protocols similar to those shown in A, and the data represent the difference in current measured in the absence and presence of NMDG or Mg^{2+}.

Ba^{2+} permeability (Dingledine et al., 1999). For example, mutations of NR1(N616) to Q, G, or W markedly reduced Ba^{2+} permeability and an N-to-R mutation had an even larger effect. Mutations of NR2B(W607) to L, N, or A, but not to Y or F, reduced Ba^{2+} permeability, highlighting the importance of an aromatic ring (as found in W, Y, and F) at this position. An NR2B(W559L) mutation had a small effect on Ba^{2+} permeability but two other mutations at this position had no effect. All of the other key mutants that were studied had no effect on Ba^{2+} permeability (Fig. 9). This highlights the specificity of these mutations and indicates that these residues are determinants of block by TB-3-4 and MK-801 but not of Ba^{2+} permeability.

Discussion

In this study, we have identified residues in several regions of NMDA receptor subunits that differentially affect block by MK-801, memantine, and TB-3-4. A model that summarizes this work is shown in Fig. 10. The model is based, in part, on previous studies in which solvent-accessible residues were probed with MTS reagents after cysteine substitution (Kuner et al., 1996; Beck et al., 1999). The M2 segment of NR1 was proposed to contain an α-helix terminating at N616 followed by an extended structure or random coil (Kuner et al., 1996). The critical asparagines in the M2 loop of NR1 and NR2B form the binding sites for Mg^{2+} and contribute to the narrow constriction of the pore (Wollmuth et al., 1996; Wollmuth et al., 1998a,b).

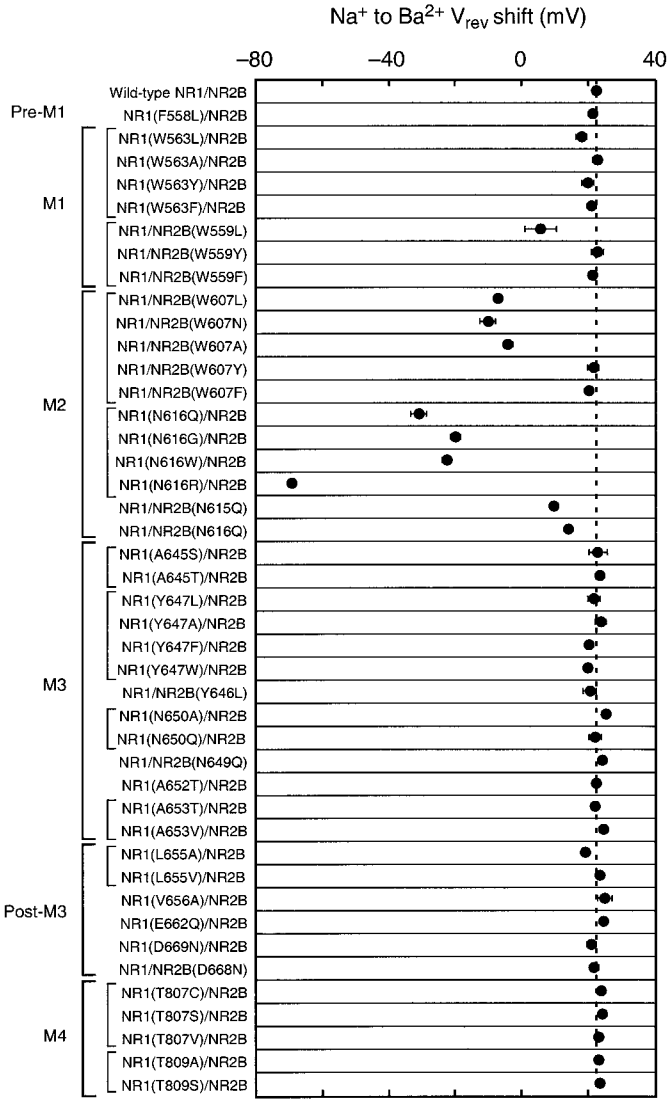

Fig. 9. Ba^{2+} permeability at NMDA channels. The shifts in reversal potential seen when currents were measured in Ba^{2+} saline versus Na^{+} saline were determined at wild-type and mutant NR1/NR2B receptors. Different mutations at the same position are grouped by thin vertical bars on the left. Thick vertical bars group residues within the various regions (M1, M2, M3, etc.). Data for some mutants in the M2 region are from Williams et al. (1998).

The model is also related to the known structure of the KcsA potassium channel (Doyle et al., 1998). There is some amino acid homology between the M2 loops of glutamate receptor subunits and the pore helix of KcsA, although in the case of NMDA receptor subunits, the homology is very limited (Fig. 11). It is possible that the M1 through M3 region of NMDA receptors has a structure similar to KcsA; M1 corresponds to the outer helix and M3 to the inner helix of KcsA. Indeed, secondary structure prediction of these regions of NR1 and NR2B suggests the presence of α helices in M1, M2, and M3 (Fig. 11). KcsA channel subunits have a pore-forming loop containing an α helix followed by a random coil; this structure may be similar to the M2 loop region of glutamate receptor subunits (Panchenko et al., 2001). Notably, the secondary structure predicted for NR1 has an M2 helix that ends just before N616, consistent with the model proposed by Kuner et al. (1996). A shorter helix is predicted in the M2 region of NR2B (Fig. 11). In this context, it is notable that there is very little amino acid identity between the M2 regions of NR1 and NR2B. It is thus conceivable that the pore loops in NR1 and NR2B are somewhat different in terms of their structure, length, or positioning within the pore. Compared with KcsA, NMDA receptor subunits contain another putative helix, M4, so the overall packing and arrangement of the membrane spanning helices in glutamate receptor subunits may be different from those in KcsA.

Mutations at the critical asparagines in M2 (N616 in NR1, N615 and N616 in NR2B) had marked effects on block by MK-801 and memantine and modest effects on block by TB-3-4. It is likely that these residues interact with the amino group of MK-801 and memantine and, possibly, with one of the amino groups of TB-3-4. The effects of mutations at NR1(N616) and NR2B(N615) were additive, suggesting that they make separate contributions to a binding site for the blocker. Some *N*-site mutations not only reduced the affinity but also increased the apparent permeation of TB-3-4 and memantine, similar to effects on block by N^1-dansyl-spermine (Chao et al., 1997). Mutations such as NR1(N616G) presumably increase the size of the narrow constriction, allowing the cationic blockers to actually permeate the channel when the driving force is sufficiently large. The values of $z\delta$ for TB-3-4 and memantine at wild-type receptors were 1.38 and 0.89, respectively. Assuming that only one molecule of each blocker binds within the transmembrane electrical field, this would correspond to δ values of 0.46 for TB-3-4 and 0.89 for memantine. TB-3-4 is a long and highly flexible molecule. If it bound in the channel in an extended conformation, then the positive charges might be distributed over some distance and it is difficult to strictly interpret the δ values as a depth of field for this molecule. In the case of memantine, it is possible that two molecules of memantine bind simulta-

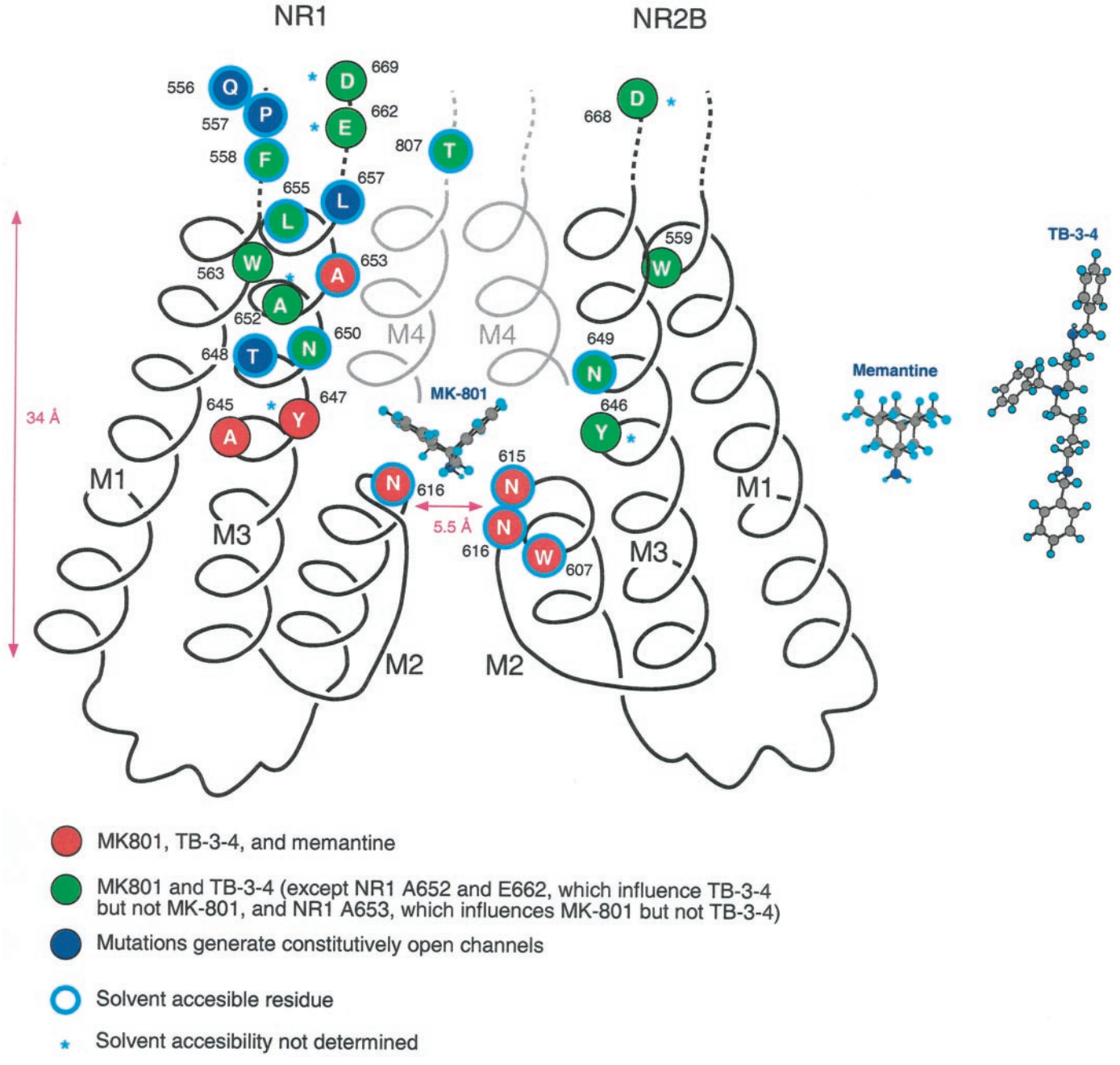

Fig. 10. Modeling residues that affect blockers in the pore and vestibule region of the NMDA receptor. The M1–M2–M3 region is depicted as a helix–pore-loop–helix similar to the structure reported for the KcsA potassium channel (Doyle et al., 1998). The M2 region contains a helix followed by a random coil structure, with the critical asparagines (N616 in NR1 and N615 in NR2B) at the tip of the helix. Only the top half of each M4 helix is shown, and the position of these helices (for which there is no equivalent in KcsA) relative to M1–M2–M3 is uncertain. Red circles indicate residues at which mutations affect block by MK-801, TB-3-4, and memantine. Green circles indicate residues at which mutations affect block by MK-801 and TB-3-4 but not by memantine. Dark blue circles are residues at which mutations generate constitutively open channels. Circles outlined in light blue indicate residues that, when mutated to cysteine, were reactive with MTS reagents and are presumed to be solvent-exposed within the lumen of the channel (Kuner et al., 1996; Beck et al., 1999). Blue asterisks indicate residues at which solvent accessibility has not been determined. Residue N649 in NR2B is assumed to be solvent accessible because the equivalent residue (N650) in NR1 is solvent accessible. Although only two subunits are shown, the receptor is most probably a tetramer or a pentamer containing two NR1 and two NR2 subunits. MK-801 is shown, drawn to scale, inside the channel, with the amino group positioned near NR1(N616) and NR2B(N615). The structures of memantine and TB-3-4 are shown adjacent to the model for comparison with MK-801. In these structures, carbon atoms are gray, hydrogen atoms are light blue, and nitrogen atoms are dark blue.

neously within the channel (Sobolevsky and Koshelev, 1998). This would yield an average δ value of 0.45 for memantine, consistent with the tip of the helix being located about halfway across the membrane electrical field (Fig. 10).

We have shown previously that mutations at NR2B(W607) alter block and permeation of extracellular Mg^{2+} (Williams et al., 1998). The effects of the NR2B(W607) mutants seen in the present study were reminiscent of their effects on block and permeation of Mg^{2+}, with an aromatic residue at this position being important for block by the organic blockers. Mutations at the equivalent residue in NR1, W608, have little or no effect. We suggested previously that NR2B(W607)

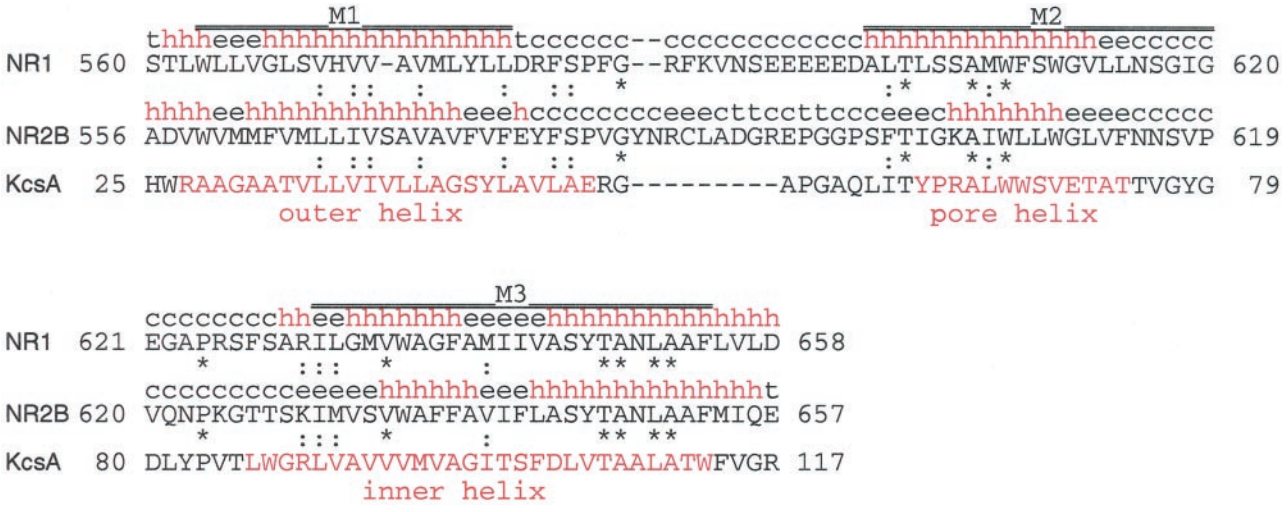

Fig. 11. Sequences of NR1 and NR2B in the M1 through M3 regions aligned with KcsA. Colons indicate similar residues in all three sequences; asterisk indicate identical residues. Sequence alignment was performed using CLUSTAL W. The segments originally designated M1, M2, and M3 are shown by lines above the sequences. Secondary structure prediction was carried out using SOPMA (http://pbil.ibcp.fr/) and is indicated above the amino acid sequences: h, α-helix (shown in red); e, extended strand; t, β turn; c, random coil. Residues in KcsA that form the outer, inner, and pore helices are shown in red.

may contribute directly to the narrow constriction and Mg^{2+} binding site (Williams et al., 1998). In this case, it could also contribute to the binding site for organic channel blockers such as MK-801, TB-3-4, and memantine (Fig. 10). Another possibility is that NR2B(W607) forms part of a structural backbone that is important for control of the pore structure. There is a conserved tryptophan in an equivalent position in KcsA (W67), the side chain of which is not exposed to the lumen of the channel but forms part of a cuff of aromatic residues that constrain the opening of the channel pore (Doyle et al., 1998).

In addition to M2, the other regions in which we identified residues that influence channel block were the pre-M1, M1, M3, post-M3, and pre-M4 regions. In the model (Fig. 10), the channel is shown as a structure with a pore formed by the helix and random coil in M2 and an outer vestibule formed by the M3 and post-M3 segments. The pre-M1 and M4 regions may also contribute to the vestibule (Beck et al., 1999). The helices are proposed to span a membrane distance of 34 Å with the dimension of the narrow constriction being 5.5 Å (Villarroel et al., 1995; Wollmuth et al., 1996). Thus, in this model, it is possible to show the relative positions of residues along each helix, but the relative positioning of residues between helices is uncertain and the relative positions of residues that lie in random coil structures (e.g., in the pre-M1 and post-M3 regions) is unknown. In addition to residues that affect sensitivity to blockers, we identified several mutations that generate constitutively open NMDA channels. The largest effects were seen with mutations at T648 in M3, but mutations at Q556 and P557 in M1 and L657 in M3 also had effects (Fig. 10, dark blue circles). These mutants presumably affect gating of the channel. Residue T648 is near residue A653, which is equivalent to a residue in the δ2 channel (an "orphan" channel related by sequence homology to glutamate receptors) at which an A-to-T mutation generates constitutively open channels responsible for the *Lurcher* mouse phenotype (Zuo et al., 1997). A-to-T mutations at NR1(A653) or NR2B(A652) do not generate constitutively open channels (K. Williams, unpublished observations), but the effects of the T648 mutants suggest that the M3 region in NMDA receptors is, like the equivalent region in δ2, important for channel gating.

Many, but not all, of the residues identified in the current study that influence channel blockers were previously shown to be exposed in the channel lumen (Kuner et al., 1996; Beck et al., 1999). The side chains of residues that are exposed to the lumen could interact directly with channel blockers, forming part of their binding sites. It is possible that residues N650, Y647, and possibly A653 in NR1, and Y646 and N649 in NR2B interact directly with MK-801 and TB-3-4 (Fig. 10). At least some of these residues are solvent exposed and positioned at a level such that MK-801 and TB-3-4 could interact with their side chains and simultaneously interact with the N residues in M2. In particular, NR1(N650) may bind to an amino group of TB-3-4 because an N-to-A mutation reduces the affinity for TB-3-4, whereas an N-to-D mutation increases affinity. The roles of residues at the top of M1 and M3 and in the pre-M1 and post-M3 regions are more difficult to interpret. Mutations at residues NR1(W563) and NR2B(W559) had pronounced effects on block by MK-801 and TB-3-4, but these residues were reported to not be solvent exposed (Beck et al., 1999). We found that an aromatic residue (W, Y, or F) at these positions was important for block by MK-801 and TB-3-4. The aromatic residue may be important for stabilizing the channel structure and/or stabilizing a binding site within the channel. Also, it seems unlikely that MK-801 (drawn to scale on Fig. 10) could interact directly with residues at the top of the M1 and M3 helices while simultaneously interacting with the M2 asparagines, although a direct interaction of TB-3-4 with these residues is conceivable.

Clearly, there are many residues that affect block by MK-801 but do not affect block by memantine (Fig. 10, green circles). Memantine and MK-801 have a similar overall size and both are influenced by the critical asparagines in M2. It is unlikely that differences in the effects of the M1, M3, and M4 mutants can be explained on the basis of the sizes of MK-801 versus memantine. However, MK-801 contains ben-

zyl rings and is more likely to make hydrophobic interactions with aromatic residues in the pore. It is possible that some residues that influence MK-801 (but not memantine) do so by altering access of the blocker to its binding site or by allosteric disruptions of the binding site. It is also possible that some mutants that influence two or more antagonists do so indirectly or allosterically rather than by directly altering side chains (or the positioning of backbone peptide groups) within the binding site. However, the mutations at these positions do not simply have general nonspecific effects on the pore structure, evidenced by their lack of effect on block by memantine and Mg^{2+} and their lack of effect on Ba^{2+} permeability.

Acknowledgment

We are grateful to Dr. A. Shirahata for supplying TB-3-4.

References

Anson LC, Chen PE, Wyllie DJA, Colquhoun D, and Schoepfer R (1998) Identification of amino acid residues of the NR2A subunit that control glutamate potency in recombinant NR1/NR2A NMDA receptors. *J Neurosci* **18:**581–589.

Beck C, Wollmuth LP, Seeburg PH, Sakmann B, and Kuner T (1999) NMDAR channel segments forming the extracellular vestibule inferred from the accessibility of substituted cysteines. *Neuron* **22:**559–570.

Blanpied TA, Boeckman FA, Aizenman E, and Johnson JW (1997) Trapping channel block of NMDA-activated responses by amantadine and memantine. *J Neurophysiol* **77:**309–323.

Chao J, Seiler N, Renault J, Kashiwagi K, Masuko T, Igarashi K, and Williams K (1997) N^1-Dansyl-spermine and N^1-(*n*-octanesulfonyl)-spermine, novel glutamate receptor antagonists: block and permeation of *N*-methyl-D-aspartate receptors. *Mol Pharmacol* **51:**861–871.

Chen H-SV, Pellegrini JW, Aggarwal SK, Lei SZ, Warach S, Jensen FE, and Lipton SA (1992) Open channel block of *N*-methyl-D-aspartate (NMDA) responses by memantine: therapeutic advantage against NMDA receptor-mediated neurotoxicity. *J Neurosci* **12:**4427–4436.

Collingridge GL and Lester RAJ (1989) Excitatory amino acid receptors in the vertebrate central nervous system. *Pharmacol Rev* **41:**143–210.

Dingledine R, Borges K, Bowie D, and Traynelis SF (1999) The glutamate receptor ion channels. *Pharmacol Rev* **51:**7–61.

Doyle D, Cabral JM, Pfuetzner RA, Kuo A, Gulbis JM, Cohen SL, Chait BT, and MacKinnon R (1998) The structure of the potassium channel: molecular basis of K^+ conduction and selectivity. *Science (Washington, D C.)* **280:**69–77.

Ho SN, Hunt HD, Horton RM, Pullen JK, and Pease LR (1989) Site-directed mutagenesis by overlap extension using the polymerase chain reaction. *Gene* **77:**51–59.

Huettner JE and Bean BP (1988) Block of *N*-methyl-D-aspartate-activated current by the anticonvulsant MK-801: selective binding to open channels. *Proc Natl Acad Sci USA* **85:**1307–1311.

Igarashi K, Shirahata A, Pahk AJ, Kashiwagi K, and Williams K (1997) Benzylpolyamines: novel, potent *N*-methyl-D-aspartate receptor antagonists. *J Pharmacol Exp Ther* **283:**533–540.

Kuner T, Wollmuth LP, Karlin A, Seeburg PH, and Sakmann B (1996) Structure of the NMDA receptor channel M2 segment inferred from the accessibility of substituted cysteines. *Neuron* **17:**343–352.

Kuryatov A, Laube B, Betz H, and Kuhse J (1994) Mutational analysis of the glycine-binding site of the NMDA receptor: structural similarity with bacterial amino acid-binding proteins. *Neuron* **12:**1291–1300.

Kutsuwada T, Kashiwabuchi N, Mori H, Sakimura K, Kushiya E, Araki K, Meguro H, Masaki H, Kumanishi T, Arakawa M, et al. (1992) Molecular diversity of the NMDA receptor channel. *Nature (Lond)* **358:**36–41.

Laube B, Hirai H, Sturgess M, Betz H, and Kuhse J (1997) Molecular determinants of agonist discrimination by NMDA receptor subunits: analysis of the glutamate binding site on the NR2B subunit. *Neuron* **18:**493–503.

Leonard JP and Kelso SR (1990) Apparent desensitization of NMDA responses in *Xenopus* oocytes involves calcium-dependent chloride current. *Neuron* **2:**53–60.

Low C-M, Zheng F, Lyuboslavsky P, and Traynelis SF (2000) Molecular determinants of coordinated proton and zinc inhibition of *N*-methyl-D-aspartate NR1/NR2A receptors. *Proc Natl Acad Sci USA* **97:**11062–11067.

Masuko T, Kashiwagi K, Kuno T, Nguyen ND, Pahk AJ, Fukuchi J, Igarashi K, and Williams K (1999) A regulatory domain (R1–R2) in the amino terminus of the *N*-methyl-D-aspartate receptor: effects of spermine, protons, and ifenprodil, and structural similarity to bacterial leucine/isoleucine/valine binding protein. *Mol Pharmacol* **55:**957–969.

Monyer H, Sprengel R, Schoepfer R, Herb A, Higuchi M, Lomeli H, Burnashev N, Sakmann B, and Seeburg PH (1992) Heteromeric NMDA receptors: molecular and functional distinction of subtypes. *Science (Wash DC)* **256:**1217–1221.

Moriyoshi K, Masu M, Ishii T, Shigemoto R, Mizuno N, and Nakanishi S (1991) Molecular cloning and characterization of the rat NMDA receptor. *Nature (Lond)* **354:**31–37.

Panchenko VA, Glasser CR, and Mayer ML (2001) Structural similarities between glutamate receptor channels and K^+ channels examined by scanning mutagenesis. *J Gen Physiol* **117:**345–359.

Paoletti P, Perin-Dureau F, Fayyazuddin A, Goff AL, Callebaut I, and Neyton J (2000) Molecular organization of a zinc binding N-terminal modulatory domain in a NMDA receptor subunit. *Neuron* **28:**911–925.

Sakurada K, Masu M, and Nakanishi S (1993) Alteration of Ca^{2+} permeability and sensitivity to Mg^{2+} and channel blockers by a single amino acid substitution in the *N*-methyl-D-aspartate receptor. *J Biol Chem* **268:**410–415.

Sayers JR, Krekel C, and Eckstein F (1992) Rapid high-efficiency site-directed mutagenesis by the phosphorothioate approach. *Biotechniques* **13:**592–596.

Sobolevsky A and Koshelev S (1998) Two blocking sites of amino-adamantane derivatives in open *N*-methyl-D-aspartate channels. *Biophys J* **74:**1305–1319.

Villarroel A, Burnashev N, and Sakmann B (1995) Dimensions of the narrow portion of a recombinant NMDA receptor channel. *Biophys J* **68:**866–875.

Williams K (1993) Ifenprodil discriminates subtypes of the *N*-methyl-D-aspartate receptor: selectivity and mechanisms at recombinant heteromeric receptors. *Mol Pharmacol* **44:**851–859.

Williams K, Pahk AJ, Kashiwagi K, Masuko T, Nguyen ND, and Igarashi K (1998) The selectivity filter of the *N*-methyl-D-aspartate receptor: a tryptophan residue controls block and permeation of Mg^{2+}. *Mol Pharmacol* **53:**933–941.

Williams K, Russell SL, Shen YM, and Molinoff PB (1993) Developmental switch in the expression of NMDA receptors occurs in vivo and in vitro. *Neuron* **10:**267–278.

Wollmuth LP, Kuner T, and Sakmann B (1998a) Adjacent asparagines in the NR2-subunit of the NMDA receptor channel control the voltage-dependent block by extracellular Mg^{2+}. *J Physiol (Lond)* **506:**13–32.

Wollmuth LP, Kuner T, and Sakmann B (1998b) Intracellular Mg^{2+} interacts with structural determinants of the narrow constriction contributed by the NR1-subunit in the NMDA receptor channel. *J Physiol (Lond)* **506:**33–52.

Wollmuth LP, Kuner T, Seeburg PH, and Sakmann B (1996) Differential contribution of the NR1- and NR2A-subunits to the selectivity filter of recombinant NMDA receptor channels. *J Physiol (Lond)* **491:**779–797.

Wong EHF, Kemp JA, Priestley T, Knight AR, Woodruff GN, and Iversen LL (1986) The anticonvulsant MK-801 is a potent *N*-methyl-D-aspartate antagonist. *Proc Natl Acad Sci USA* **83:**7104–7108.

Woodhull AM (1973) Ionic blockage of sodium channels in nerve. *J Gen Physiol* **61:**687–708.

Zuo J, DeJager PL, Takahashi KA, Jiang W, Linden DJ, and Heintz N (1997) Neurodegeneration in Lurcher mice caused by mutation in δ2 glutamate receptor gene. *Nature (Lond)* **388:**769–773.

Address correspondence to: Dr. Keith Williams, Department of Physiology and Pharmacology, SUNY Health Science Center, Brooklyn, 450 Clarkson Avenue, Box 31, Brooklyn, NY 11203-2098. E-mail: keithwnyc@mindspring.com